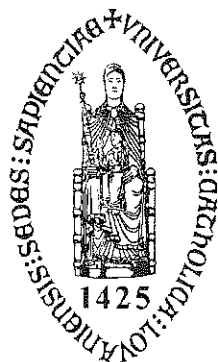


KATHOLIEKE UNIVERSITEIT LEUVEN

**DEPARTEMENT INTERFASECHEMIE
CENTRUM VOOR OPPERVLAKTECHEMIE EN KATALYSE**



**FOURTH MEETING
OF THE
BENELUX EPR SOCIETY**

Book of Abstracts

Organizers :

Bert M. Weckhuysen and Robert A. Schoonheydt

**May 24 1996
Arenbergkasteel
Heverlee
Belgium**

Scientific Programme

10.00-10.25 : Registration & Coffee

10.25-10.30 : Opening Remarks

10.30-11.30 : *Invited Lecture* : F.E. Mabbs, University of Manchester, U.K.

"Multi-frequency c.w. EPR spectra of copper(II)dimers"

11.30-12.00 : *Lecture L1* : D.E. De Vos, Katholieke Universiteit Leuven

"Fine structure in the EPR spectra of Mn exchanged on zeolite A"

12.00-12.30 : *Lecture L2* : R.J. Hulsebosch, Universiteit Leiden

"Control of radical pair lifetime by microwave irradiation"

12.30-14.00 : Lunch

14.00-14.30 : *Lecture L3* : O.G. Poluektov, Universiteit Leiden

"The electronic structure of the shallow boron acceptor in 6H-SiC : A pulsed EPR/ENDOR study at 95 GHz."

14.30-15.00 : *Lecture L4* : P.J. van Dam, Universiteit Nijmegen

"Pulsed EPR investigations of 'Fe-only' hydrogenase from *D. vulgaris* and *M. elsdenii*."

15.00-15.30 : *Lecture L5* : R.A.J. Janssen, Universiteit Eindhoven

"High-spin m-p-aniline oligo(cation radical)s"

15.30-16.00 : General Meeting of the Benelux EPR Society

16.00-17.30 : Poster Session & Coffee

Poster P1 : S. De Vries, Universiteit Delft, The Netherlands

"Molybdopterin radical in aldehyde oxidoreductase"

Poster P2 : A.W. Bosman, Universiteit Eindhoven, The Netherlands

" Proxyl functionalized dendrimers"

Poster P3 : W.S. Kijlstra, Universiteit Amsterdam, The Netherlands

"Alumina supported manganese oxides : an EPR characterization study"

Poster P4 : B.M. Weckhuysen, Katholieke Universiteit Leuven, Belgium

"Multi-frequency EPR spectroscopy of zeolite encapsulated copper(II) amino acid complexes"

Poster P5 : E.J. Reijerse, Universiteit Nijmegen, The Netherlands

"Simulation strategies for N-14 ESEEM spectra in the regime of perturbation theory : application to oxobis(2-methylquinolin-8-olato)vanadium (IV)"

Poster P6 : P.J. van Dam, Universiteit Nijmegen, The Netherlands

"ESEEM and ENDOR investigations of Cu(II)-bleomycin and two model complexes"

Poster P7 : E.J. Reijerse, Universiteit Nijmegen, The Netherlands

"ESEEM studies of oxobis(salicyl-aldoxime)vanadium(IV) : determination of the sign of the nitrogen hyperfine coupling"

Poster P8 : R. Heidler, Katholieke Universiteit Leuven, Belgium

"EPR lineshape of Mn²⁺ in the incommensurately modulated phase of betaine calcium chloride dihydrate (BCCD) - simulation and experiment"

**Abstracts
of
Lectures and Posters**

MULTI-FREQUENCY C.W.EPR SPECTRA OF COPPER(II) DIMERS

Frank E. Mabbs

EPSRC c.w.EPR Service Centre, Chemistry Department, University of Manchester, Manchester,
M13 9PL, United Kingdom

The magnetic susceptibilities and EPR spectra of Copper(II) dimers have continued to be of interest since the first report of such studies on copper acetate monohydrate. Magnetic susceptibility measurements are the preferred method of measuring the intra-molecular singlet-triplet separation (expressed via the exchange parameter J), although such information can be obtained from EPR. The magnitude and sign of J depends upon the structural details of an individual dimer. In an isolated dimer the triplet state may be split by fine structure, Zeeman and hyperfine interactions expressed by the spin-Hamiltonian : $H = D[S_z - 1/3S(S+1)] + E[(S_x)^2 - (S_y)^2] + \beta.B.g.S + S.A.I.$

An analysis of the EPR spectra of such systems as either frozen solutions, single crystals or undiluted powders permits the determination of the spin-Hamiltonian parameters. In the solid state the presence of surrounding dimers may have an effect on the EPR spectrum. Thus dipolar and inter-dimer exchange interactions may result in line broadening with subsequent loss of copper hyperfine structure. However, the temperature variation of the line broadening permits the estimation of the inter-dimer exchange. A further complication which may arise from inter-dimer exchange is the appearance of features additional to those predicted by the above spin-Hamiltonian. These additional features are most easily detected in powder spectra where they usually occur at g_{eff} around 2 and with temperature dependent intensities. A number of recently prepared dimeric copper(II) compounds, with differing types of bridging arrangements, which exhibit some or all of the above effects will be discussed.

Fine Structure in the EPR spectra of Mn exchanged on zeolite A

Dirk E. De Vos,^{†*} Bert M. Weckhuysen* and Thomas Bein[†]

[†] Chemistry Department, Purdue University, IN 47906 West Lafayette, USA

* Center for Surface Science and Catalysis, K.U.Leuven, Belgium.

In this presentation, ESR spectroscopy is used to gain insight in the siting of divalent manganese in zeolites with the LTA topology. X and Q band spectra of Mn were recorded for Li⁺, Na⁺, K⁺, Cs⁺ and NH₄⁺ zeolites, at different Mn concentrations and temperatures. In total six different species were identified in the spectra. These species have widely varying values for the zero-field splitting (ZFS) parameters. For some species, the deviation from cubic symmetry is limited, and only the central $M_S = -\frac{1}{2} \leftrightarrow \frac{1}{2}$ transition is observed. Magnitudes for the ZFS parameter D can then be derived for example from the intensity of the forbidden $\Delta M_S = \pm 1$, $\Delta M_L = \pm 1$ lines. In other cases, there is a well-defined and rather large zero-field splitting. As a consequence, all the $\Delta M_S = \pm 1$ transitions between the six electronic states of the d^5 ion are observed, and the ZFS parameter D can be derived directly from this fine structure. Temperature sometimes strongly affects the spectra, as the value and the distribution of the D parameter may be very temperature dependent.

The Mn speciation is shown to be primarily determined by the co-cation present on the zeolite. In the hydrated state, Mn exchanged K⁺, Cs⁺ and NH₄⁺ A zeolites display similar spectra with $D = 0.036 \text{ cm}^{-1}$, suggesting that the size of these co-cations causes steric crowding in the large cages of zeolite A. Very different spectra are obtained with hydrated Li⁺ and Na⁺ zeolites: part of the Mn assumes an almost octahedral coordination ($D < 0.01 \text{ cm}^{-1}$), but for some of the Mn ions, the coordination sphere is subject to a very pronounced axial distortion ($D = 0.15 \text{ cm}^{-1}$, $E \approx 0$). These parameters are then related to data obtained from X-ray diffraction studies. For instance, the strong axial distortion of the Mn coordination geometry in NaA and LiA may be related to a trigonal bipyramidal site, which has been inferred from X-ray data. In such a site, Mn occupies the center of a six-ring window of a sodalite cage, with two water molecules in the apical positions.

An analogous approach was followed to describe the Mn species in the dehydrated zeolites. The dehydration - rehydration cycles are perfectly reversible and allow to study the interconversion of the various Mn species. Finally the present results are compared with data for other Mn zeolites, such as faujasites, and with data for other cations, such as Cu²⁺, in zeolites with LTA topology.

CONTROL OF RADICAL PAIR LIFETIME BY MICROWAVE IRRADIATION

Hulsebosch, R.J. and Gast, P.

Huygens Laboratorium, Universiteit Leiden, Postbus 9504, 2300 RA Leiden, The Netherlands

Radicals produced by illumination or ionizing radiation are often produced in pairs, which quickly decay by recombination or by diffusion and subsequent reactions. For maximizing the yield of products, and for facilitating the study of reaction pathways, it is desirable to minimize the probability of radical pair recombination. We present a way to control the radical pair lifetime through the application of resonant microwaves in the presence of a magnetic field. Herewith, two radical pair triplet states are populated, from which the pair cannot recombine directly to the singlet ground state because of spin conservation. We illustrate the method with a photosynthetic photochemical reaction, where we have achieved an increase in radical pair lifetime of up to two orders of magnitude.

• THE ELECTRONIC STRUCTURE OF THE SHALLOW BORON ACCEPTOR IN 6H-SiC:
A PULSED EPR/ENDOR STUDY AT 95 GHz.

O.G.Poluektov, M.Matsumoto, P.G.Baranov and J.Schmidt

Huygens Laboratory, University of Leiden, P.O.Box 9504,
2300 RA Leiden, The Netherlands
Fax: 31-71-5275819, E-mail: mfgo@ruihl1.leidenuniv.nl

Boron is the most important shallow acceptor in SiC and its electronic structure has been studied intensively in the last 30 years. The theoretical model for the B-shallow acceptor has been reinterpreted several times. EPR experiments on a ^{13}C -enriched 6H-SiC crystal established that B replaces Si and that it occupies 3 sites with equal probability: two quasi cubic (k_1 and k_2) and one hexagonal (hex) [1]. In the model proposed by Zubatov et al [1] the main spin density was located on the dangling bond of a C atom along the C-B connection line. In more recent publications [2-4] a new description was given on the basis of ENDOR and ODMR investigations. In this model the valence electron is donated to B by a neighboring C atom thus forming a $\text{B}_{\text{Si}}^- - \text{C}^+$ bond. The unpaired electron of C^+ is uniformly distributed among the three remaining bonding orbitals. The authors call this model the boron-induced carbon acceptor.

In this contribution we present the results of a high-frequency (95 GHz) EPR and ENDOR study of the shallow B acceptor in a ^{13}C -enriched 6H-SiC crystal. The high spectral resolution of this technique allows us to measure accurately the g-tensor of all shallow B sites. Moreover we studied the hyperfine tensors of the ^{11}B and the ^{13}C nuclear spin of the neighboring C atom. The results allow us to build a consistent model for the electronic structure of the shallow B acceptor in 6H-SiC which explains all magnetic resonance data.

We conclude that the main spin density of the unpaired electron is located on the B-C bond as originally suggested by Zubatov et al [1]. From a ^{29}Si and ^{13}C ENDOR study it is further concluded that 60-70 % of the spin density is distributed in the crystal with a Bohr radius of 2.2 \AA , a value that is in reasonable agreement with effective mass theory.

References.

1. A.G.Zubatov, I.M.Zaritskii, S.N.Lukin, E.N.Mokhov and V.G.Stepanov. Sov.Phys.Solid State **27** (1985) 197.
2. R.Müller, M.Feege, S.Greulich-Weber and J.-M.Spaeth, Semicond.Sci.Technol. **8** (1993) 1377.
3. J.Reinke, R.Müller, M.Feege, S.Greulich-Weber and J.-M.Spaeth, Mat.Sc.Forum, **143-147** (1994) 63.
4. F.J.Adrian, S.Greulich-Weber, J.-M.Spaeth, Solid State Comm., **94** (1995) 41.

Pulsed EPR investigations of "Iron-Only" Hydrogenases: A histidine residue is involved in the deactivation of the H-cluster

† Pieter J. van Dam, Eduard J. Reijerse and Wilfred R. Hagen

Department of Molecular Spectroscopy, University of Nijmegen, Toernooiveld 1, 6525 ED Nijmegen, The Netherlands.

Hydrogenases are metallo-enzymes involved in redox reactions with molecular hydrogen. They use hydrogen as receptor or donor with the basic reaction: $H_2 \rightleftharpoons 2H^+ + 2e^-$. The active H-cluster of the "Iron-only" hydrogenases from *M. elsdenii* and *D. vulgaris* has been investigated with ESEEM and HYSCORE spectroscopy. In both proteins the coordination of nitrogen nuclei to the cluster was confirmed. One set of quadrupole interaction parameters ($K = 4.83$ MHz, $\eta = 0.13$) is similar to that measured on hydrogenase obtained from *C. pasteurium*. The high quadrupole coupling constant suggests coordination of an unusual type of nitrogen. Taking into account that a diatomic cofactor has been found for other hydrogenases we propose that a small cofactor, i.e. N_2 or CN^- must be present.

The inactivated hydrogenase from *D. vulgaris* (generated by O_2 or CO exposure) shows ^{14}N -ESEEM signals which are consistent with an imidazole interaction. Its parameters are similar to those measured on Rieske type iron-sulfur clusters. Since a histidine nearby the cluster is conserved in the known amino acid sequences of Fe-hydrogenases the assumption is made that this histidine plays a role in the hydrogen reduction/oxidation. The inactivation of the enzyme is thus accompanied by the coordination of the imidazole ring to the H-cluster.

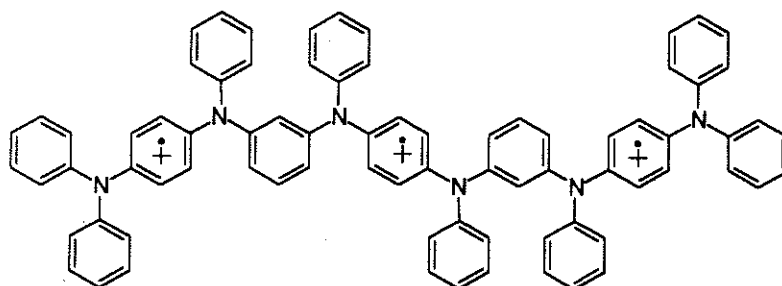
HIGH-SPIN *M-P*-ANILINE OLIGO(CATION RADICAL)S

M. M. Wienk and R. A. J. Janssen

Laboratory of Organic Chemistry, Eindhoven University of Technology, PO Box 513, 5600 MB Eindhoven, The Netherlands

A promising strategy towards organic oligomers and polymers with a high-spin ground state is the concept of a polaronic ferromagnetic chain, based on an alternating sequence of dopable π -conjugated segments and ferromagnetic spin coupling units. A major problem encountered in the experimental verification of this concept has been the lack of stability of open-shell π -conjugated segments under ambient conditions.

We now report on series of new aniline and *N*-phenylaniline oligomers that consist of alternating *para* and *meta* substituted phenylene rings which can be easily oxidized to the corresponding oligo(cation radical)s. These structures have been synthesized to meet two important criteria for future organic ferromagnets, i.e.: chemical stability from the *p*-diaminobenzene unit and ferromagnetic coupling from the *m*-diaminobenzene unit.



The oligo(cation radical)s are investigated using EPR spectroscopy and zero field splittings are obtained. Variable temperature experiments down to 3.8 K demonstrate that the high-spin state corresponds to the ground state. In addition to EPR, we have used UV/Vis/NIR spectroscopy, cyclic voltammetry, and electrospray mass spectrometry to assess the electronic structure in detail.

We conclude that *m-p*-aniline oligo(cation radical)s are chemically stable under ambient conditions and possess a high-spin ground state when the oxidation level is adjusted to one charge per *p*-diaminobenzene unit. We have been able to generate triplet and quartet state cation radicals with intramolecular ferromagnetic interactions in one and two dimensions.

MOLYBDOPTERIN RADICAL IN ALDEHYDE OXIDOREDUCTASE FROM COMAMONAS TESTOSTERONI

S. de Vries, D.M.A.M. Luykx and J.A. Duine

Department of Microbiology and Enzymology, Delft University of Technology,
Julianalaan 67, 2628 BC Delft, The Netherlands

Enzymes containing the Mo- or W-pterin cofactor are widespread in nature; they occur in eubacteria, archaeobacteria and in lower and higher eukaryotes. A thoroughly studied example is Xanthine oxidase from cow milk. The enzyme is a homodimer (300 kDa) and contains in addition to the Mo-pterin cofactor, one FAD group and two, EPR distinguishable, [2Fe-2S] centers. The Mo-pterin serves as the site of substrate binding and oxidation, a process in which the molybdenum changes its redox state from Mo(VI) to Mo(IV). The Mo(IV) is subsequently oxidized in two single-electron transfer steps with the paramagnetic Mo(V) as intermediate. The precise pathway of electron transfer is unknown, but rapid-mixing rapid-quenching experiments suggest that the four redox centers are in rapid electronic equilibrium. Taking the structure of Xanthine oxidase as the structural archetype of these enzymes, many variants are found, in particular in prokaryotes. The prokaryotic enzymes generally consist of three subunits, which together cover the sequence of the single, large, subunit of Xanthine oxidase. Some enzymes, however, consist of only two subunits, e.g. lacking the flavin-containing subunit. There is also variation in the structure of the pterin cofactor, i.e. in prokaryotes a nucleotide diphosphate (G, A, C or H) instead of a single phosphate group is attached to the pterin ring system.

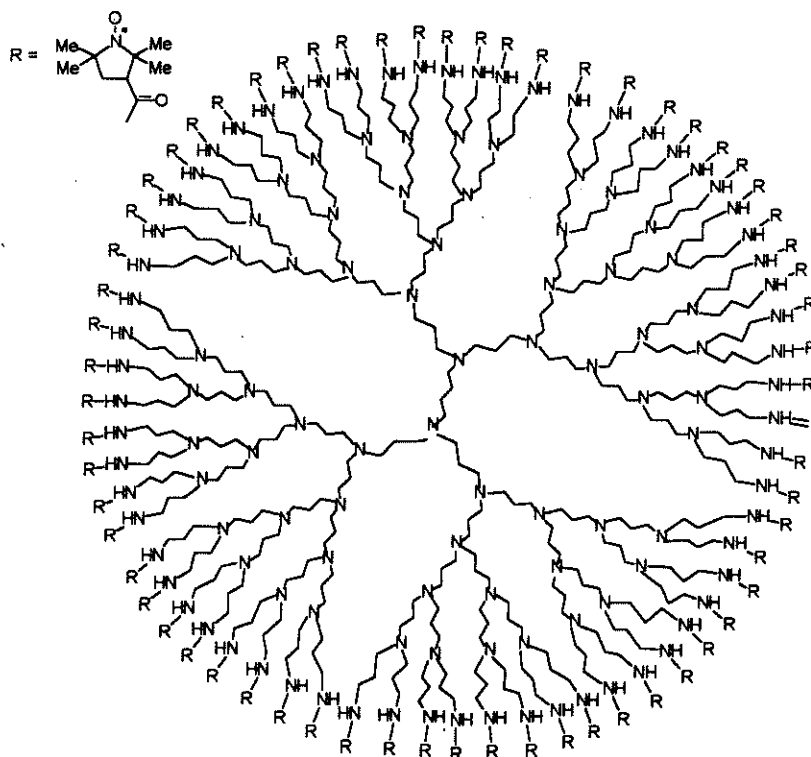
Very recently, the 3D-structure of two pterin-containing enzymes have been determined, of Aldehyde ferredoxin oxidoreductase from *Pyrococcus furiosus* containing W-pterin and of Aldehyde oxidoreductase from *Desulfovibrio gigas* with the Mo-pterin cofactor. Two new findings emerge from that work. The pterin cofactor is a non-planar three-ringed structure and not a two-ringed system. In the Aldehyde ferredoxin oxidoreductase the W-ion is coordinated by two pterin molecules. The Aldehyde oxidoreductase from *Comamonas testosteroni* studied in this work consists of three subunits, contains one Mo-pterin cytosine dinucleotide, one FAD and two different [2Fe-2S] centers and is structurally similar to the Aldehyde oxidoreductase from *D. gigas*. This latter enzyme lacks, however, the FAD-containing subunit. The EPR spectrum of partially and completely reduced Aldehyde oxidoreductase from *C. testosteroni* shows two different [2Fe-2S] clusters, but no signals of Mo(V) or a FAD-radical owing to a high disproportionation constant. The EPR spectrum of the enzyme as isolated (viz. oxidized) shows a novel type of signal, not observed in other Molybdoproteins. The signal is due to a $S = 1/2$ system, consists of six approximately equally-spaced lines, has $g = 2.004$ and is apparently isotropic both at X-band and Q-band frequencies. Although these properties are reminiscent of an organic free radical, the finding that the EPR spectrum cannot be observed at room temperature but starts to broaden at temperatures above 60K suggests a more complicated structure. Substitution of natural Mo with ^{95}Mo and ^{98}Mo showed a slight increase in the linewidth in the sequence ^{98}Mo , $^{\text{nat}}\text{Mo}$, ^{95}Mo , consistent with an interaction between the $S=1/2$ and the $I=5/2$ from the Mo nucleus. Substitution of ^{14}N with ^{15}N affected the shape and resolution of the spectrum and substitution of H_2O for D_2O changed the six-line spectrum to a four-line spectrum, suggesting the presence of two exchangeable protons. All these properties strongly suggest that the EPR signal is due to a Mo-monohydropterin radical. Its possible role in the mechanism of action of the enzyme will be discussed.

PROXYL FUNCTIONALIZED DENDRIMERS

A. W. Bosman, R. A. J. Janssen, and E. W. Meijer

Laboratory of Organic Chemistry, Eindhoven University of Technology, PO Box 513, 5600 MB Eindhoven, The Netherlands

Dendrimers or cascade molecules are highly branched three-dimensional macromolecules, synthesized stepwise from a central core leading to a well-defined number of generations and end groups. We set out to investigate the dynamical behavior of these molecules in solution by introducing nitroxyl spin labels as end groups. Here we report the preparation and structural investigation using EPR spectroscopy of poly(propylene imine) dendrimers up to the fifth generation, functionalized with respectively 2, 4, 8, 16, 32, or 64 3-carboxyproxyl end groups. The EPR spectra of these polyproxyl radicals are strongly temperature and solvent dependent. This allowed studying the dynamical behavior of these molecules. At higher temperatures and in aprotic polar solvents the spectra are dominated by a large exchange ($J \gg a_N$) interaction between the proxyl radicals giving rise to well-defined multiplets in the EPR spectrum from thermally populated high-spin states. For dendrimers with 2 to 8 proxyl groups, the spectral resolution is sufficient to simply count the number of end-groups from the spectra. For higher generations the overall spectral shape is consistent with the expected polyradical structure.



*Fifth generation proxyl functionalized dendrimer
(DAB-dendr-(NH-3-carboxyproxyl)₆₄)*

Alumina supported Manganese Oxides: an ESR Characterisation Study

W. Sjoerd Kijlstra¹, Eduard K. Poels¹, Alfred Blik¹, Bert M. Weckhuysen², Robert A. Schoonheydt².

¹ Institute of Chemical Engineering, University of Amsterdam, Nieuwe Achtergracht 166, 1018 WV Amsterdam.

² Center for Surface Chemistry and Catalysis, KU Leuven, Kardinaal Mercierlaan 92, 3001 Heverlee.

Alumina supported manganese oxides are reported¹ as very active catalysts for the selective catalytic reduction (SCR) of NO with NH₃. The catalysts are prepared by incipient wetness impregnation with a Mn(CH₃COO)₂ solution. This method results in a highly dispersed MnO_x layer, as no XRD diffraction lines are observed up to 6 wt% Mn loading. However, the selectivity of the catalysts towards N₂ production already decreases sharply between 2 and 4.5 wt% Mn loading, suggesting the formation of twodimensional MnO_x clusters responsible for the undesired side reactions (non selective catalytic reduction of NO to N₂O and NH₃ oxidation). As ESR is able to detect paramagnetic Mn species, it is used to study the relation between isolated and clustered Mn species quantitatively as a function of loading.

Results indicate that up to 4.5 wt% Mn loading the intensities of the ESR signals (integrated over the whole magnetic field range applied) follow the Curie-Weiss law; at 7 wt% a significant deviation of this behaviour is observed. The intensity of the ESR signal at 0.5 wt % loading shows that more than 90% of the Mn-species is isolated at that loading. The ESR signals normalized on the amount of Mn decrease sharply up to 4.5 wt% Mn and remain constant at higher loadings. These results show that up to 4.5 wt% Mn loading at least part of the Mn species is isolated. However, the contribution of clusters to the ESR-signal increases sharply between 0.5 and 4.5 wt%. At 7 wt% Mn, only clusters are present.

The ESR spectra consist of a central hyperfine sextet with additional lines at higher and lower field, suggesting an axially distorted symmetry. The fine structure is superimposed by a very broad band indicating that the spectrum is composed by signals of at least two paramagnetic Mn species. As the average oxidation state of Mn is 3.1, as determined by TPR, both Mn²⁺ and Mn⁴⁺ can be present at the surface and their signals can contribute to the ESR spectra.

Future research objectives are the evaluation of the nature of the Mn-species giving rise to the ESR spectrum (with appropriate g-, A- and D-values) by simulation with the programm QPOW. If the spectra are composed of a Mn²⁺ and a Mn⁴⁺ contribution attempts will be made to quantify those contributions, thus describing the fractions Mn²⁺, Mn³⁺ and Mn⁴⁺ quantitatively. Subsequently, spectra after adsorption of NO, NH₃ and H₂O at low temperatures (298-423 K) will be recorded to reveal if (and possibly how) these SCR reactants and products can penetrate the first coordination sphere of the Mn species during reaction conditions.

¹ L. Singoredjo, R.B. Korver, F. Kapteijn, J.A. Moulijn, Appl. Catal. B, 1 (1992) 297.

MULTI-FREQUENCY EPR SPECTROSCOPY OF ZEOLITE ENCAPSULATED COPPER(II) AMINO ACID COMPLEXES

Bert M. Weckhuysen*, An A. Verberckmoes, Lijun Fu and Robert A. Schoonheydt

Centrum voor Oppervlaktechemie en Katalyse, Departement Interfasechemie, K.U.Leuven, Kardinaal Mercierlaan 92, 3001 Heverlee (Leuven), Belgium

Cu(amino acid) complexes represent mimics of the active center of natural Cu-enzymes, which are known to be the most abundant, active and selective catalysts in nature. Enzyme mimicking is the building of the active center of enzymes into an inorganic matrix, such as zeolites, which allows a larger operational temperature domain in a broader spectrum of solvents. Here, we report on the characterization of zeolite encapsulated $\text{Cu}(\text{AA})_n^{m+}$ -complexes (with AA = amino acid) by combined X- and Q-band cw EPR spectroscopies.

The AA's investigated are lysine, glycine, alanine, serine, proline, tyrosine, histidine, glutamine, glutamic acid, cysteine, tryptophane, leucine and arginine, but stable $\text{Cu}(\text{AA})_n^{m+}$ -complexes are only obtained with arginine, lysine, histidine and proline. Independently of the Cu-loading and the ligand type, the hydrated $\text{Cu}(\text{AA})_n^{m+}$ -samples are characterized by a typical axially symmetric spectrum with hyperfine splitting in EPR with g_{\parallel} and g_{\perp} and A_{\parallel} values around respectively 2.25, 2.06 and 175 G. This is summarized in table 1, together with the EPR parameters of Cu exchanged zeolite Y as a reference material. The EPR parameters were obtained by spectrum simulation.

Table 1. ESR parameters of Cu-Y and immobilized $\text{Cu}(\text{AA})_n$ complexes in zeolite Y.

Zeolite	g_{\parallel}	g_{\perp}	A_{\parallel} (G)	A_{\perp} (G)	$A_{\perp,N}$ (G)
$[\text{Cu}(\text{H}_2\text{O})_6]^{2+}$ -Y	2.40	2.09	134	9	-
$[\text{Cu}(\text{lysine})_2]^{2+}$ -Y	2.24	2.06	179	9	-
$[\text{Cu}(\text{arginine})_2]^{2+}$ -Y	2.24	2.06	180	9	-
$[\text{Cu}(\text{histidine})_2]^{+}$ -Y (at low loadings)	2.27	2.06	178	9	13
$[\text{Cu}(\text{histidine})_2]^{+}$ -Y (at high loadings)	2.24	2.05	183	9	-
$[\text{Cu}(\text{proline})^{+}]$ -Y (species A)	2.31	2.06	160	9	-
(species B)	2.41	2.09	132	9	-

Simulation strategies for ^{14}N ESEEM spectra in the regime of perturbation theory.

Edward J. Reijerse¹, Alexei M. Tyryshkin² and Sergei A. Dikanov³

(1) Department of Molecular spectroscopy, University of Nijmegen, Toernooiveld, 6525 ED Nijmegen (The Netherlands). (2) Institute of Chemical Kinetics and Combustion, Novosibirsk 630090, Russia, (3) Current address: MS and D, Pacific Northwest Laboratories, Richland, WA 99352, USA

A ^{14}N -ESEEM simulation strategy based on first and second order perturbation analysis of peak positions is presented and applied to the ESEEM data of the complex: Oxobis(2-methylquinolin-8-olato) Vanadium(IV) ($\text{VO}(\text{meox})_2$). Making use of the information in the orientation selection ESEEM and HYSORE spectra the number of free fitting tensor parameters can be reduced from 9 to 4 (i.e. the α and β Euler angles of both HFI and NQI interaction matrices). Further constraints based on local symmetry of the complex enable to reduce the number of free parameters to 2. It turns out that the best fit parameter space for this complex is consistent with its crystal structure data. The NQI tensor is near axial and pointing in the ligand plane. The hyperfine interaction is weakly anisotropic and one axis is oriented perpendicular to the ligand plane.

A "HYSCORE" investigation of oxobis(salicyl-aldoxime) Vanadium (IV). Characterization of nitrogen coordination and intramolecular hydrogen bonding.

Edward J. Reijerse¹ and Jesús I. Martínez^{1,2}.

(1) Department of Molecular spectroscopy, University of Nijmegen, Toernooiveld, 6525 ED Nijmegen (The Netherlands). (2) Instituto de Ciencia de Materiales de Aragón, Universidad de Zaragoza-Consejo Superior de Investigaciones Científicas. Pza. S. Francisco s/n, 50009 Zaragoza (Spain).

Electron Spin Echo Envelope Modulation (ESEEM) is a powerful technique for the study of small hyperfine interactions occurring in biologically interesting metal complexes. Coupling of electron with surrounding nuclei gives information about the structure and activity of such compounds. However, it is usually difficult to get single crystals of these complexes. Interpretation of ESEEM spectra from polydomain (powder) samples is difficult because of superposition of signals corresponding to all possible orientations as well as of the modulation intensity anisotropy. Multifrequency and 2D-ESEEM allows to overcome some of these difficulties.

We will present a multifrequency and 2-D ESEEM (HYSCORE) study of a model oxovanadium complex (VO)(Salox)₂. Our one and two dimensional ESEEM measurements cover the range of C- and X-band frequencies. We take advantage of the possibility of measuring either polydomain or orientation-selective spectra. From that we obtain information about the distance of intramolecular protons (hydrogen bonds) to the metal and about the value of the nitrogen spin coupling parameters. Furthermore, we demonstrate the possibility of utilizing the proton-nitrogen cross-correlation features in 2D-ESEEM to determine the relative signs of the hyperfine interactions.

EPR line shape of Mn^{2+} in the incommensurately modulated phase of Betaine Calcium Chloride Dihydrate (BCCD)—Simulation and Experiment

R. Heidler*, H. Metz† and W. Windsch†

* Centrum voor Oppervlaktechemie en Katalyse, Kotholieke Universiteit Leuven, Kard. Mercierlaan 92, B-3001 Heverlee

† Fakultät für Physik und Geowissenschaften, Universität Leipzig, Linnéstraße 5, D-04103 Leipzig

Betaine Calcium Chlorid Dihydrat, BCCD, $(CH_3)_3N^+CH_2COO^-CaCl_2 \cdot 2H_2O$ belongs to the famous ferroelectric compounds formed by an α -amino acid and an inorganic adduct, like for instance trisarcosine calcium chloride (TSCC) and triglycine sulfate (TGS). BCCD exhibits beside a paraelectric high temperature phase ($T_I = 164$ K) and a ferroelectric low temperature phase ($T_C = 46.5$ K) a series of commensurately and incommensurately modulated phases forming an incomplete devils staircase. The main interest in this substance lies in the incommensurately modulated phases IC1 (between 164 K and 124 K) and IC2 (between 122 K and 118 K).

The EPR spectrum of Mn^{2+} substituting Ca^{2+} can be described by the following Spin-Hamiltonian:

$$\begin{aligned}\hat{H} &= \hat{H}_{Zeeman} + \hat{H}_{FS} + \hat{H}_{HFS} \\ &= g\beta\vec{B}_0\vec{S} + \vec{S}D\vec{S} + a_{iso}\vec{S}\vec{I} \\ &= g\beta\vec{B}_0\vec{S} + D[S_z^2 - \frac{1}{3}S(S+1)] + E[S_x^2 - S_y^2] + a_{iso}\vec{S}\vec{I}\end{aligned}\quad (1)$$

with the following values for the parameters:

g	2.00
$\frac{D}{g\beta}$	-958.5 G
$\frac{E}{g\beta}$	32 G
$\frac{A}{g\beta}$	-92.5 G

Due to the strong fine structure splitting it is not possible to interpret the EPR spectrum on the basis of the perturbation theory. Therefore we used for the interpretation of these spectra the exact diagonalization of the Spin-Hamiltonian. So it is possible to determine not only the magnitude of the axial fine structure splitting constant D but also its relative sign compared with the (negative assumed) hyperfine structure splitting constant. On the basis of these simulations we are able to interpret also the EPR-line shape in the first incommensurately modulated phase of BCCD assuming two modulated tiltings of the fine structure tensor, a relatively large one about the Z-axis of the fine structure tensor (amplitude 40° for $T = T_I - 10$ K) and a small one about its Y-axis (amplitude 5° for $T = T_I - 10$ K).

List of Registered Participants

Abdelhamid B., Centrum voor Oppervlaktechemie en Katalyse, K.U.Leuven, Kardinaal Mercierlaan 92 3001 Heverlee, Belgium

Bosman A., Laboratorium van Organische Scheikunde, Technische Universiteit Eindhoven, PO Box 513, 5600 MB Eindhoven, The Netherlands

Cos P., Laboratorium voor Farmaceutische Microbiologie, Universiteit Antwerpen, Universiteitsplein 1, 2610 Antwerpen, Belgium

De Boer E., Departement Moleculaire Spectroscopie, Faculteit Wetenschappen, Universiteit Nijmegen, Toernooiveld, 6525ED, Nijmegen, The Netherlands

Debuyst R., Laboratoire de Chimie Inorganique et Nucléaire, 2 Chemin du Cyclotron, 1348 Louvain-la-Neuve, Belgium

Dejehet F., Laboratoire de Chimie Inorganique et Nucléaire, 2 Chemin du Cyclotron, 1348 Louvain-la-Neuve, Belgium

De Vos D., Centrum voor Oppervlaktechemie en Katalyse, K.U.Leuven, Kardinaal Mercierlaan 92 3001 Heverlee, Belgium

De Vries S., Department of Microbiology and Enzymology, Delft University of Technology, Julianalaan 67, 2628 BC Delft, The Netherlands

Driessen M., Departement Moleculaire Spectroscopie, Faculteit Wetenschappen, Universiteit Nijmegen, Toernooiveld, 6525ED, Nijmegen, The Netherlands

Fremout A., Laboratorium voor Kristallografie en studie van de vaste stof, Vakgroep vaste stofwetenschappen, Universiteit Gent, Krijgslaan 281/S1, 9000 Gent, Belgium

Gast P., Huygens Laboratorium, Universiteit Leiden, Postbus 9504, 2300 RA Leiden, The Netherlands

Goovaerts E., Departement Fysica, Universitaire Instelling Antwerpen, Universiteitsplein 1, 2610 Antwerpen, Belgium

Grobet P., Centrum voor Oppervlaktechemie en Katalyse, K.U.Leuven, Kardinaal Mercierlaan 92, 3001 Heverlee, Belgium

Hagen W., Departement Moleculaire Spectroscopie, Faculteit Wetenschappen, Universiteit Nijmegen, Toernooiveld, 6525ED, Nijmegen, The Netherlands

Heidler R., Centrum voor Oppervlaktechemie en Katalyse, K.U.Leuven, Kardinaal Mercierlaan 92 3001 Heverlee, Belgium

Hulsebosch R., Huygens Laboratorium, Universiteit Leiden, Postbus 9504, 2300 RA Leiden, The Netherlands

- Ikoma, T., Huygens Laboratorium, Universiteit Leiden, Postbus 9504, 2300 RA Leiden, The Netherlands
- Janssens G., Centrum voor Oppervlaktechemie en Katalyse, K.U.Leuven, Kardinaal Mercierlaan 92 3001 Heverlee, Belgium
- Janssen R., Laboratorium van Organische Scheikunde, Technische Universiteit Eindhoven, PO Box 513, 5600 MB Eindhoven, The Netherlands
- Kaess H., Departement Fysica, Universitaire Instelling Antwerpen, Universiteitsplein 1, 2610 Antwerpen, Belgium
- Kijlstra S., Instituut Chemische Ingenieurswetenschappen, Universiteit Amsterdam, Nieuwe Achtergracht 166, 1018 WV Amsterdam, The Netherlands
- Klaassen A., Departement Moleculaire Spectroscopie, Faculteit Wetenschappen, Universiteit Nijmegen, Toernooiveld, 6525ED, Nijmegen, The Netherlands
- Knops-Gerrits P., Centrum voor Oppervlaktechemie en Katalyse, K.U.Leuven, Kardinaal Mercierlaan 92 3001 Heverlee, Belgium
- Maes F., Laboratorium voor Kristallografie en studie van de vaste stof, Vakgroep vaste stof-wetenschappen, Universiteit Gent, Krijgslaan 281/S1, 9000 Gent, Belgium
- Mabbs F., Chemistry Department, University of Manchester, Manchester, M13 9PL, United Kingdom
- Mouithys-Mickalad A., Center of the Biochemistry of Oxygen, Institute of Chemistry B-6, Sart-Tilman Univeristy of Liège, 4000 Liège, Belgium
- Nulens K., Centrum voor Oppervlaktechemie en Katalyse, K.U.Leuven, Kardinaal Mercierlaan 92 3001 Heverlee, Belgium
- Poluektov O., Huygens Laboratorium, Universiteit Leiden, Postbus 9504, 2300 RA Leiden, The Netherlands
- Priem A., Departement Moleculaire Spectroscopie, Faculteit Wetenschappen, Universiteit Nijmegen, Toernooiveld, 6525ED, Nijmegen, The Netherlands
- Reijerse E., Departement Moleculaire Spectroscopie, Faculteit Wetenschappen, Universiteit Nijmegen, Toernooiveld, 6525ED, Nijmegen, The Netherlands
- Schoofs B., Centrum voor Oppervlaktechemie en Katalyse, K.U.Leuven, Kardinaal Mercierlaan 92 3001 Heverlee, Belgium
- Schoonheydt R., Centrum voor Oppervlaktechemie en Katalyse, K.U.Leuven, Kardinaal Mercierlaan 92 3001 Heverlee, Belgium
- Schosseler P., Laboratorium für Physikalischen Chemie, ETH-Zentrum, Universitätstrasse 22/G33, CH-8092 Zürich, Switzerland
- Sels B., Centrum voor Oppervlaktechemie en Katalyse, K.U.Leuven, Kardinaal Mercierlaan 92 3001 Heverlee, Belgium

Struijk M., Laboratorium van Organische Scheikunde, Technische Universiteit Eindhoven, PO Box 513, 5600 MB Eindhoven, The Netherlands

Szweryn W., Departement Moleculaire Spectroscopie, Faculteit Wetenschappen, Universiteit Nijmegen, Toernooiveld, 6525ED, Nijmegen, The Netherlands

Tadaaki I., Huygens Laboratorium, Universiteit Leiden, Postbus 9504, 2300 RA Leiden, The Netherlands

Van Boxtel H., Laboratorium van Organische Scheikunde, Technische Universiteit Eindhoven, PO Box 513, 5600 MB Eindhoven, The Netherlands

Van Dam P., Departement Moleculaire Spectroscopie, Faculteit Wetenschappen, Universiteit Nijmegen, Toernooiveld, 6525ED, Nijmegen, The Netherlands

Van Doorslaer S., Laboratorium für Physikalischen Chemie, ETH-Zentrum, Universitätstrasse 22/G33, CH-8092 Zürich, Switzerland

Van Haare J., Laboratorium van Organische Scheikunde, Technische Universiteit Eindhoven, PO Box 513, 5600 MB Eindhoven, The Netherlands

Vrielinck H., Laboratorium voor Kristallografie en studie van de vaste stof, Vakgroep vaste stofwetenschappen, Universiteit Gent, Krijgslaan 281/S1, 9000 Gent, Belgium

Weckhuysen B., Centrum voor Oppervlaktechemie en Katalyse, K.U.Leuven, Kardinaal Mercierlaan 92 3001 Heverlee, Belgium

Wienk M., Laboratorium van Organische Scheikunde, Technische Universiteit Eindhoven, PO Box 513, 5600 MB Eindhoven, The Netherlands

Zdravkova M., Laboratorium voor Kristallografie en studie van de vaste stof, Vakgroep vaste stofwetenschappen, Universiteit Gent, Krijgslaan 281/S1, 9000 Gent, Belgium